# Cystathionine-β-synthase affects organization of cytoskeleton and modulates carcinogenesis in colorectal carcinoma cells

**Veronika Liskova**
Biomedical Research Center of the Slovak Academy of Sciences: Biomedicinske centrum Slovenskej akademie vied
**Barbora Chovancova**
Biomedical Research Center of the Slovak Academy of Sciences: Biomedicinske centrum Slovenskej akademie vied
**Petr Babula**
Faculty of Medicine, Masaryk University, Brno
**Ingeborg Rezuchova**
Biomedical Research Center of Slovak Academy of Sciences
**Kristina Ploth Pavlov**
Biomedical Research Center of the Slovak Academy of Sciences: Biomedicinske centrum Slovenskej akademie vied
**Miroslava Matuskova**
Biomedical Research Center of the Slovak Academy of Sciences: Biomedicinske centrum Slovenskej akademie vied
**Olga Krizanova** ( olga.krizanova@savba.sk )
Biomedical Research Center, Slovak Academy of Sciences

**Research**

**Keywords:** cystathionine-β-synthase, cytoskeleton, β-tubulin, colorectal carcinoma cells, tumors, proliferation

**Posted Date:** November 5th, 2020

**DOI:** https://doi.org/10.21203/rs.3.rs-100291/v1

# Abstract

**Background:** Cystathionine-b-synthase (CBS), one of three enzymes that endogenously produce hydrogen sulfide, is extensively studied for its relevance also in various tumor's cell. In our previous work we observed that immunofluorescence pattern of CBS is very similar to that from tubulin and actin. Therefore, we focused on potential interaction of CBS with cytoskeletal proteins b-actin and b-tubulin and functional relevance of the potential interaction of these proteins in colorectal carcinoma cell lines.

**Methods:** To study potential interaction of CBS with cytoskeletal proteins and its functional consequences, CBS-knockout DLD1 (DLDx) cell line was established by using the CRISPR/Cas9 gene editing method. Interaction of selected cytoskeletal protein with CBS was studied by immunoprecipitation and Western blot analysis, immunofluorescence and proximity ligation assay. Functional consequences were studied by proliferation and migration assays and by generation of xenografts in SCID/bg mice.

**Results:** We have found that CBS, an enzyme that endogenously produces $H_2S$, binds to cytoskeletal b-tubulin and to lesser extent also to b-actin in colorectal carcinoma derived cells. When CBS was knockouted by CRISPR/Cas9 technique (DLDx), we observed de-arranged cytoskeleton compared to unmodified DLD1 cell line. Treatment of these cells with a slow sulfide donor GYY4137 resulted in normal organization of cytoskeleton, thus pointing to the role of CBS in microtubule dynamics. To evaluate the physiological importance of this observation, both DLD1 and DLDx cells were injected into SCID/bg mice and size/mass of developed xenografts was evaluated. Significantly larger tumors developed from DLDx compared to DLD1 cells, which correlated with increased proliferation of these cells.

**Conclusions:** Taken together, in colorectal cancer DLD1 cells, CBS binds to cytoskeleton, modulates microtubule dynamics and thus affects the proliferation and migration in colorectal carcinoma stable cell line.


# Background

Cystathionine-b-synthase (CBS) is one of three enzymes that endogenously produce hydrogen sulfide ($H_2S$). $H_2S$ is a relatively novel gaseous transmitter, to which several regulatory roles were already attributed. CBS is localized both, in cytoplasm and mitochondria [1] and is regulated by variety of physiological factors, e.g. 1,25-dihydroxyvitamin D3, hypoxia-inducible factors, estradiol-17b, etc. (for review see [2]), depending on a type of cells. Physiological role of CBS is still not completely clear, although detrimental effect on the cardiovascular system is evident [3]. Permanent CBS gene knockdown in immortalized human adipose-derived mesenchymal stem cells promoted a cellular senescence phenotype with increased adipogenic potential and excessive lipid storage [4]. Also, regulation of immune and inflammatory responses by CBS was described [5].

Expression of the CBS was studied in several types of tumors. Increased levels of CBS were detected in colon/colorectal cancer [6, 7], papillary carcinoma [8], breast and also in prostate cancer [9]. This enzyme was increased also in thyroid malignancies [10]. However, decrease in CBS expression was determined in

clear cell renal cell carcinoma that is spontaneously hypoxic, compared to matched controls and this decrease was dependent on the grade of tumor [8]. Question remains, whether higher CBS levels in tumors could be due to lower amount of $H_2S$ in tumor, as it was suggested by Dongsoo et al. [11]. Bell-shaped model has been proposed to explain the role of $H_2S$ in cancer development. Specifically, endogenous $H_2S$ or a relatively low level of exogenous $H_2S$ may exhibit a pro-cancer effect, whereas exposure to $H_2S$ at a higher amount or for a long period may lead to cancer cell death [12]. In favor of this hypothesis might be a fact, that slow sulfide donor GYY4137 can induce apoptosis in stable cancer cell lines *in vitro*, but also in xenografts induced in immunodeficient mice treated with GYY4137 [13, 14].

Role of CBS in carcinogenesis was studied on various types of tumors by several laboratories using different approaches. In ovarian cancer cells, CBS regulates bioenergetics by regulating mitochondrial ROS production, oxygen consumption and ATP generation [15]. Inhibition of CBS can improve ovarian cancer treatment [16]. In colon cancer – derived epithelial cell lines a role for endogenous $H_2S$ in tumor angiogenesis was shown [6]. In breast cancer, CBS-derived $H_2S$ might play a role in the protection of breast cancer cells against activated macrophages [17].

CBS was shown to be localized mainly in cytosol and to a lesser extend in mitochondria [18, 19]. However, few years ago we have shown a specific CBS pattern by immunofluorescent staining [8], similar to staining of cytoskeleton. Thus, we built up a hypothesis that CBS might bind to cytoskeletal proteins.

Microtubules are major cytoskeletal components in the eukaryotic cells. Microtubules and microtubule dynamics is involved in several important activities, like maintenance of cell shape and cell motility, cell division and accurate chromosome segregation during mitosis, general intracellular communication and intracellular tracking of macromolecules and organelles in the interphase. In cancer cells, a high expression of several b-tubulin isotypes correlated with aggressive clinical behavior, chemotherapy drug resistance, and also poor prognosis [20]. Cytotoxic action of microtubule-targeting drugs (such as taxanes or vinca alkaloids) is based on the variations of microtubule dynamics. Modulation of microtubules can significantly affect the fate of cells. Chaudhuri and co-workers [21] have shown that tubulin disulfides may play a role in tubulin folding and that thiol-disulfide exchange in tubulin could be a key regulator in microtubule assembly and dynamics of tubulin *in vivo*. Under physiological conditions, tubulins are sulfhydrated, which affects the microtubule assembly [22]. Also, Hosono et al. [23] showed the effect of diallyl trisulfide (DATS) on modification of cysteins Cys-12b and Cys-354b in b-tubulin, which is assumed to be a cause for the disruption of microtubule network formation. Nevertheless, microtubule assembly is dependent on variety other factors (e.g. acetylation, GTP, phosphorylation) and a mutual interplay of all these factors should be also considered.

Based on the current knowledge on CBS and also our previous experiments we aimed to study potential interaction of CBS and some cytoskeletal proteins, i.e. b-actin and b-tubulin (while this type of tubulin has binding sites for taxanes, vinca alkaloids, etc.[24]). Since cytoskeleton is crucially involved in carcinogenesis and also is a target of some groups of chemotherapeutics, functional relevance of the potential interaction with CBS was studied as well.

# Material And Methods

## Cell cultivation and treatments

Experiments were performed on colorectal carcinoma cell lines DLD1 (CCL-221, ATCC, Sigma-Aldrich, St. Louis, MO, USA) and HCT116 (CCL-247, ATCC, Sigma-Aldrich), line derived from clear cell renal cell carcinoma (ccRCC) (ECACC, 03112702, Sigma-Aldrich) and non-cancerous cell line derived from epithelial cells – EA.hy926 (ATCC, CRL-2922TM). Cell lines were cultured in RPMI medium (Sigma-Aldrich) or Dulbecco Minimal Essential Medium (DMEM; Sigma-Aldrich) with a high glucose (4.5 g/L) and L-glutamine (300 µg/mL), supplemented with 10% fetal bovine serum (Sigma-Aldrich) and penicillin/streptomycin mixture (Calbiochem, San Diego, CA, USA; penicillin 100U/mL; streptomycin 100 µg/mL). Cells were treated with paclitaxel (PTX; Selleckchem, Pittsburgh, PA, USA; 20 nmol/L), vincristine sulfate salt (Vin; Sigma-Aldrich; 100 nmol/L) a slow-releasing sulfide donor GYY4137 (GYY; Cayman Chemical, Ann Arbor, MI, USA; 10 µmol/L), for 24 h.

## Generation of CBS-knockout DLD1 cell line

CBS-knockout DLD1 cell line, hereafter referred DLDx, was established by using the CRISPR/Cas9 (CRISPR (clustered, regularly interspaced, short palindromic repeats)/Cas9 (CRISPR-associated protein 9)) gene editing method. The CBS CRISPR guide RNA sequences (GATTTCGTTCTTCAGCCGCC and TGTGCCCTCAGGGATCGGGC) were designed by the laboratory of Feng Zhang at the Broad Institute in order to efficiently target the CBS gene with minimal risk of off-target Cas9 binding elsewhere in the genome [25, 26]. Lentiviral transfer plasmids lentiCRISPRv2_CBS-1 and lentiCRISPRv2_CBS-3 (GenScript, Leiden, Netherlands) contained a lentiCRISPRv2 backbone and single above-mentioned oligos cloned into the single guide RNA (sgRNA) scaffold. To produce lentiviral particles, transfer plasmids lentiCRISPRv2_CBS-1 or lentiCRISPRv2_CBS-3 were co-transfected into HEK293T cells with the packaging plasmids pMD2.G (Addgene, Watertown, MA, USA) and psPAX2 (Addgene). Virus-containing medium was collected after 48, 60, and 72 h and passed through a 0.45 µm low protein-binding filter. Lentiviruses were concentrated using PEG 6000 and sedimented by centrifugation (1500 × g, 4°C for 30 min). As a positive control to monitor transduction efficiency, CRISPR-lenti human EMX1 positive control transduction particles (CRISPR11V-1EA, Sigma-Aldrich) were used. Similarly, as a negative control, CRISPR-lenti non-targeting control transduction particles (CRISPR12V-1EA, Sigma-Aldrich) were used. This control includes a guide RNA sequence that does not target known human, mouse and rat genes. DLD1 cells, plated the day before at a density of $0.25\times10^5$ cells per 6 cm plate, were infected with each lentivirus, or their combination. DLD1 cells transducted by control lentivirus particles were called DLD-PC (positive control) and DLD-NC (negative control). Twenty-four hours after transduction, cells were selected by puromycin (Puromycin, InvivoGen, USA) and then the CBS protein knockout was confirmed by immunofluorescence (IF) and Western blot analysis (WB).

## Immunofluorescence

Cells grown on glass coverslips were fixed in ice-cold methanol. Nonspecific binding was blocked by incubation with PBS containing 3% bovine serum albumin (BSA; Sigma- Aldrich) for 60 min at a room temperature. Cells were then incubated with primary antibodies diluted in PBS with 1% BSA (PBS-BSA) for 1 h at 37°C. The antibody specific to human CBS (1:100 dilution, AP6959c, Abgent, San Diego, CA, USA), the anti-beta tubulin antibody (1:1000 dilution, ab231082, Abcam, Cambridge, UK) and the anti-beta actin antibody (1:250 dilution, ab6276, Abcam) were used. Afterwards, cells were washed four-times with PBS with 0.02% TWEEN (Sigma-Aldrich) for 10 min, incubated with Alexa Fluor-594 goat anti-mouse/anti-rabbit (1:1000 dilution, Thermo Fisher Scientific, Waltham, MA, USA) or IgG Alexa Fluor-488 donkey anti-rabbit IgG (1:1000 dilution, Thermo Fisher Scientific) in PBS-BSA for 1 h at 37°C, and washed as described previously. Finally, cover-slips were mounted onto slides in mounting medium with a blue-fluorescent DNA stain 4',6-diamidino-2-phenylindole (DAPI, Sigma-Aldrich). Cells were visualized by epifluorescence microscopy using Nikon Eclipse Ti-S/L100 (Nikon, Japan); NIS elements software (Nikon, Tokyo, Japan) was used to process images and to evaluate the resultant pictures.

### Proximity Ligation Assay

The proximity ligation assay (PLA) was used for *in situ* detection of the co-localization between CBS and b-tubulin or b-actin. The assay was performed in a humid chamber at 37°C according to the manufacturer's instructions (Olink Bioscience, Uppsala, Sweden). Cells were seeded on glass coverslips and further cultured for 24 h. Afterwards, cells were fixed with methanol, blocked with 3% PBS-BSA for 30 min, incubated with a mixture of antibodies against CBS and b-tubulin or b-actin for 1 h, washed three times, and incubated with plus and minus PLA probes for 1 h. Then, the cells were washed (3x5 min), incubated for 40 min with ligation mixture containing connector oligonucleotides, washed again, and incubated with amplification mixture containing fluorescently labeled DNA probe for 100 min. After a final wash, the samples were mounted and the signal was analyzed using a Zeiss LSM 510 Meta confocal microscope with a Plan Neofluar 40_/1.3 oil objective. The following antibodies were used: human CBS (1:100 dilution, AP6959c, Abgent), the anti-beta tubulin antibody (1:1000 dilution, ab231082, Abcam) and the anti-beta actin antibody (1:250 dilution, ab6276, Abcam).

### Western blot analysis

Cells were scraped into 10 mmol/L Tris-HCl, pH 7.5, 1 mmol/L phenylmethyl- sulfonyl fluoride (PMSF, Serva, Heidelberg, Germany), protease inhibitor cocktail tablets (Complete EDTA-free, Roche Diagnostics, Indianapolis, IN, USA) and centrifuged for 5 min at 3000 x g at 4°C. Pellet was re-suspended in Tris-buffer containing the 50 µmol/L CHAPS (3-[(3-cholamidopropyl) dimethylammonio] 1-propanesulfonate, Sigma-Aldrich), and then incubated for 30 min at 4°C. Lysate was centrifuged for 15 min at 10 000 x g at 4°C. Protein concentration was determined by Modified Lowry Protein Assay Kit (Thermo Scientific). Fifteen to forty micrograms of protein extract from each sample was separated by electrophoresis on 4-20% gradient SDS polyacrylamide gels. Afterwards, proteins were transferred to Hybond PVDF blotting membrane (GE Healthcare, Life Sciences, Chicago, IL, USA) using semidry blotting (Owl, Irvine, CA, USA). Membranes were blocked in 5% non-fat dry milk in TBS-T (Tris-buffered Saline with Tween-20) for

overnight at 4°C and then incubated for 1 h with primary antibody β-actin (1:5000 dilution, ab6276, Abcam), antibody β-tubulin (1:1000, ab108348, Abcam), or membranes were blocked in 5% non-fat dry milk in TBS-T or 5% BSA in TBS-T for 1 h at room temperature and then incubated overnight at 4°C with appropriate primary antibodies: CBS (1:1000 dilution, ab144600, ab135626, Abcam), p53 (1:1000 dilution, ab154036, Abcam) and p53 phospho S20 (1:1000 dilution, ab157454, Abcam). After washing, membranes were incubated with secondary antibodies to mouse (secondary goat anti-mouse antibody; 1:10 000 dilution, ab6789, Abcam) or rabbit (secondary goat anti-rabbit antibody; 1:10 000 dilution, ab97200, Abcam) IgG conjugated to horseradish peroxidase for 1 h at room temperature. For visualization, chemiluminescence detection system (Luminata™ Crescendo Western HRP Substrate, Millipore, Burlington, Mass., USA) was used. Each membrane was digitally captured using an imaging system (C-DiGit, LI-COR).

### Immunoprecipitation

Appropriate antibody (anti-human CBS, ab135626, Abcam) was incubated with 60 µL washed magnetic beads (Dynabeads M-280), coated with M-280 sheep anti-rabbit IgG (Invitrogen Dynal AS, Oslo, Norway) for overnight at 4°C on a rotator (VWR International, Radnor, PA, USA). As negative controls, the coated beads were incubated with either mouse IgG1_ (MOPC21, Sigma, USA), or with rabbit - globulin (Jackson ImmunoResearch, West Grove, PA, USA). The beads with attached antibody were washed (twice, 200 µL) with phosphate-buffered saline (PBS). Proteins were immunoprecipitated from 0.5 mg of detergent-extracted total protein by incubation for 4 h at 4°C with antibody-bound beads. Bead complexes were washed four times with PTA solution (145 mmol/L NaCl, 10 mmol/L $NaH_2PO_4$, 10 mmol/L sodium azide, and 0.5% Tween 20, pH 7.0). Immunoprecipitated proteins were then extracted with 60 µL of 2x Laemmli sample buffer (Bio-Rad, Hercules, CA, USA) and boiled for 5 min.

### Proliferation assay

Relative viability of the cells was determined by the CellTiter-Glo™Luminescent Cell Viability Assay (Promega Corporation, Madison, WI, USA) on 96-well plate using 3000 cells per well and evaluated by the LumiStar GALAXY reader (BMG Labtechnologies, Germany) after 4 days from plating and treatment with GYY4137. Experiments were performed in octaplicates, repeated at least three times from different cultivations. Values were expressed as means ± S.E.M.

### Cell migration assay

Fifty thousand DLD1, DLDx, DLDNC and DLDPC cells per well were plated on ImageLock 96-well plates (Essen BioScience, Ann Arbor, MI, USA), and let to adhere for 24 h. Confluent monolayers were then wounded with wound needle (IncuCyteWoundMaker; Essen BioScience), washed twice and supplemented with fresh culture medium or fresh culture medium with GYY4137. Images were taken every 2 h for the next 24 h in the IncuCyte ZOOM™ kinetic imaging system (Essen BioScience). Cell migration was evaluated by IncuCyte ZOOM™ 2016A software (Essen BioScience) based on the relative wound density measurements and expressed as means of octaplicates ± S.E.M.

### Immunohistochemical staining

Paraffin-embedded tumor tissue was sliced in 5 μm sections. Tissue was pre-treated in automated water bath at 96°C for 20 min using Dako PT link (Dako, Glostrup, Denmark ). After washing in 1x Envision FLEX wash buffer (Dako), slides were incubated with FLEX peroxidase-blocking reagent (Dako) for 10 min. Sections were incubated with primary anti-human Ki67 (MIB-1 FLEX, Dako) antibody at RT for 20 min. Subsequently, sections were incubated with LSAB2 System-HRP, Biotinylated Link for 20 min and then with Streptavidin-HRP for 20 min at RT. Visualization was performed by incubation with 3,3'-Diaminobenzidine (DAB substrate-chromogen solution, Dako) for 2 min. Nuclei were counterstained with hematoxylin (FLEX, Dako, Denmark) for 5 min at RT. Among incubations, slides were washed in 1x FLEX wash buffer (Dako). The slides were mounted with Dako Faramount Aqueous Mounting Medium (Dako) and the stained sections were then analyzed by Axiovert 40C Zeiss microscope and Zen 2.6 software (Zeiss, Jena, Germany).

### In vivo experiments

Animal experiments were approved by the Institutional Ethic Committee and by the national competence authority – State Veterinary and Food Administration of the Slovak Republic (project registration No. Ro-2032-3/2020-220) in compliance with the Directive 2010/63/EU and the Regulation 377/2012 on the protection of animals used for scientific purposes. Project was conducted in the approved animal facility (license No. SK UCH 02017). SCID/bg mice (males, 17 weeks old at the beginning of experiment) were bilaterally subcutaneously injected by $1x10^6$ DLD1, DLDx, DLD-PC or DLD-NC cells resuspended in 100 μL of serum-free cultivation medium. Visible xenografts developed after 4 days. Mice were then randomly divided into either a treatment group (intraperitoneal injection of 20 mg/kg GYY4137 diluted in saline, given daily), or a control group (saline). Xenografts were measured every 3 days with a caliper, and the tumor volume (V) was calculated according to the formula: $V=length \times width^2/2$, the width being the greatest transverse diameter and length the greatest longitudinal diameter. Mice were kept on standard pelleted food and water *ad libitum*, monitored daily for the weight loss or other signs of possible toxic effects of the drug. At the experimental endpoints (after 14 days of therapy) mice were sacrificed. Xenografts were resected, weighed and cryopreserved at -80°C for further experiments or stored in buffered formaline.

### Statistical analysis

The results are presented as mean ± S.E.M. Each value represents an average of at least 3 wells from at least three independent cultivations of each type of cells. Statistical differences among groups were determined by one way ANOVA. For multiple comparisons, an adjusted t-test with p values corrected by the Bonferroni method was used (InStat, GraphPad Software). Statistical significance * or + - $p < 0.05$ was considered to be significant, ** or ++$p < 0.01$, *** or +++$p < 0.001$.

## Results

Immunofluorescence with anti-CBS antibody revealed similar staining as b-tubulin in variety of cells (Fig. 1A). This staining pattern was visible in colorectal carcinoma cell lines DLD1 and HCT116, in cell line derived from clear cell renal cell carcinoma (ccRCC) and also in non-cancerous cell line derived from epithelial cells – EA.hy926. Therefore, we built up a proposal that CBS might co-localize with b-tubulin and/or b-actin. To verify this proposal, we performed immunoprecipitation with anti-CBS antibody and subsequent immunodetection with b-tubulin and b-actin antibodies in DLD1 and HCT116 cells (Fig. 1B). We observed a clear signal with both cytoskeletal antibodies, also in the presence of slow sulfide donor GYY4137 (GYY). Further, we decided to show co-localization of these proteins by proximity ligation assay. Red dot signal shows co-localization of CBS with both, b-actin and b-tubulin (Fig. 1C). To demonstrate CBS interaction with b-tubulin, we performed double immunofluorescence with CBS (Fig. 2, red signal) and b-tubulin (green signal) in control DLD1 group, in a group of DLD1 cells treated with vincristine (that prevents polymerization of tubulin) or paclitaxel (that prevents depolymerization of tubulin). In vincristine-treated DLD1 group b-tubulin signal almost diminished, similarly to CBS signal. In paclitaxel-treated DLD1 group, both, b-tubulin signal and also CBS signal was much stronger compared to untreated group (Fig. 2), thus proving the interaction of these two proteins. Specificity of CBS and b-tubulin signals was verified by negative control (Fig. 2, inset), where primary antibodies were omitted. To study the functional role of CBS in colorectal carcinoma cells, we prepared a DLD1/CBS_del (DLDx) cell line with inactive CBS gene by CRISPR/Cas9 gene editing method. These clones were selected by puromycin selection (Fig. 3A), were we got three clones (2, 6, 7) lacking CBS. For further experiments we used clone 2 (DLDx). Absence of CBS in DLDx was demonstrated also by proximity ligation assay with b-tubulin and CBS antibodies (Fig. 3B) and immunofluorescence with CBS antibody (Fig. 3C). We also prepared positive (DLD-PC) and negative (DLD-NC) CRISPR controls to eliminate possible false results due to CRISPR manipulations (Fig. 3A). When comparing b-tubulin net in DLD1 and DLDx cells, we observed rapid differences between these two groups of cells (Fig. 4). Control group of DLD1 cells contained very well defined microtubules with regular distribution in the cells (without accumulation in some cell parts). Individual microtubules showed homogenous structure. Compared to control, signal of b-tubulin in DLDx cells was significantly weaker. The structure of microtubules was non-homogenous with presence of much brighter “spots” in their structure (Fig. 4, arrows). In these cells, microtubules showed accumulation mainly around nuclei, and on the contrary, they were almost missing at the periphery of cells, where their spot-like structure was very well evident. Application of GYY4137 led to restoration of a homogeneous distribution of microtubules as well as to the homogeneity of individual microtubules (without spot-like structure; Fig. 4). Both, DLD1 and DLDx cells were injected subcutaneously into the immunodeficient SCID/bg mice. When small tumors started to be detectable, GYY4137 treatment was applied to two groups of mice (Fig. 5). After 14 days mice were sacrificed and volume together with tumor’s weight were determined. Volume (Fig. 5A,B) and weight (Fig. 5A) of tumors were approximately twice as big in mice inoculated with DLDx than with DLD1 cells. Interestingly, when mice with DLDx tumors were simultaneously treated with GYY4137, volume and weight of tumors were significantly smaller and remained on values from DLD1 inoculated mice (Fig. 5,A,B). Injection of positive and/or negative CRISPR cell lines (DLD-PC and DLD-NC) to SCID/bg mice resulted in the same size of tumors as inoculation with DLD1 (not shown). Immunohistochemistry from tumors was performed and proliferation marker Ki-67

was determined (Fig. 5C). Slightly increased staining of Ki-67 was determined in tumors from DLDx cells compared from DLD1 cells. In mice, treated with GYY4137 a slight decrease in proliferation marker Ki-67 was detected in tumors originating from DLDx (Fig. 5C). Phosphorylation of tumor suppressor p53 at position Ser-20 was decreased in DLDx, compared to DLD1 cells, while p53 protein was in both groups of cells the same (Fig. 5D). Proliferation and migration was also significantly higher in DLDx compared to DLD1 (Fig. 6). Nevertheless, while proliferation was not affected by GYY4137 treatment neither in DLD1, nor in DLDx cells (Fig. 6A), GYY4137 decreased migration in both, DLD1 and also in DLDx cells (Fig. 6B). Control positive and negative CRISPR did not affect these processes (Fig. 6).

# Discussion

Using the cystathionine-b-synthase antibody we observed “fibred” like immunofluorescent staining in DLD1, HCT116, ccRCC and also in EA.hy926 cell, which suggest binding of CBS to cytoskeletal proteins. Immunoprecipitation with CBS antibody and subsequent Western blot analysis as well as proximity ligation assay proved that CBS binds to b-tubulin and also to b-actin. Also, we compared immunofluorescence of CBS and b-tubulin by using two microtubule targeting agents, both affecting b-tubulin – paclitaxel and vincristine (for review see [24, 27]). Paclitaxel was shown to inhibit human cervical cancer cell division at low concentrations of the drug (0.25 mM) and blocks human cervical cancer cells in the G2/M phase [28]. Immunofluorescence of DLD1 cells showed significantly increased staining of both, tubulin and CBS in paclitaxel treated cells, compared to control, untreated ones. Additionally, when we used vincristine, chemotherapeutic agent, which prevents polymerization of b-tubulin, very small signal of CBS and tubulin occurred compared to controls. These results together with previously discussed strongly suggest that CBS binds to cytoskeletal proteins in DLD1 cells.

It is obvious that binding of CBS to cytoskeletal proteins might result in functional consequences. Changes in CBS binding might participate in re-organization of cytoskeleton and potentially, to altered tumorigenicity. This proposal is based on previous observations that cysteine residues in tubulin are actively involved in regulating ligand interactions and microtubule formation both *in vivo* and *in vitro*. These cysteine residues are sensitive markers in determining the conformation of tubulin. Tubulin dimer possesses 20 cysteine residues, from which twelve are localized in α-tubulin and eight cysteins are in β-tubulin.
Nevertheless, while function of the b-tubulins in microtubule assembly is known, function of the a-tubulin isotypes in microtubule dynamics remains unknown [27]. Cysteine oxidation is usually accompanied by loss of polymerization competence. Thus, it is not clear whether these modifications are only the result of oxidative stress or whether they also function as regulators under normal conditions. Certain cysteine residues of tubulin might regulate the dimer/microtubule equilibrium and the thioredoxin system might, in turn, regulate this equilibrium [29].

To evaluate the physiological relevance of CBS in colorectal carcinoma cells, we used CRISPR/Cas9 gene editing method [25, 26] to prepare DLD1 cell line with knockouted CBS (DLDx). Efficiency of the CRISPR was determined by Western blot and hybridization with CBS antibody, by immunofluorescence and

proximity ligation assay with CBS and b-tubulin antibodies. To eliminate false results due to possible interference of CRISPR technique, we prepared also positive (DLDPC) and negative (DLDNC) CRISPR control. These controls normally expressed the CBS.

The b-tubulin immunostaining of DLDx revealed significant changes in cytoskeletal morphology compared to unmodified DLD1 cells. In DLDx cells we observed partial destruction of tubulin microfilaments, thus suggesting an important role of CBS and sulfide signaling, possibly through cysteine residues. It looks like CBS has a protective effect on microtubules. It was already shown that substitution of cysteine residues yields tubulin that is not capable for assembling into microtubules [29]. However, reduced tubulin is polymerization competent, forming normal microtubules [30]. Thus a role for the cysteines in tubulin remains unresolved. Although there are several papers discussing different role of individual isotypes of b-tubulin in carcinogenesis (for review see [27]), these isotypes have 85-95% similarity and therefore from the point of CBS binding it is difficult to recognize among them. Nevertheless, polymerization of b-tubulin is depends on wide variety of factors (e.g. phosphorylation, acetylation) and all these processes might be targeted by $H_2S$ produced by CBS. Further research is required to clarify this mechanism (which might be distinct from production of $H_2S$).

Physiological relevance of CBS/tubulin complex was studied by determining xenografts on immunodeficient SCID/bg mice, proliferation and migration. Xenografts obtained from DLDx cells were significantly larger than those from DLD1 cells. Immunohistochemistry of tumor's slices revealed increased staining of Ki-67 that points to increased proliferation in tumors from DLDx than in DLD1. Parallel treatment of mice with GYY4137 resulted in prevention of DLDx tumor's rapid growth, suggesting involvement of the $H_2S$ in this process. GYY4137 is a slow sulfide donor that release $H_2S$ slowly and steadily, either in aqueous solution or administered to the animals, because of low toxicity [31]. Effect of GYY4137 on tumor suppression was already demonstrated on DLD1 and HepG2 cells [13, 14]. In cell cultures, DLDx exhibited also increased proliferation compared to DLD1 and GYY4137 significantly decreased this process in DLDx cells, but not in DLD1 cells. Mechanism, how CBS can through cytoskeletal proteins affect tumors´ growth, proliferation and migration needs to be studied in detail. As stated by Zuhra et al. [2] – "even when the involvement of CBS in a given biological process is undisputable, it is often difficult to determine if the observed biological effects related to CBS are, in fact, due to upstream alterations (e.g., homocysteine accumulation due to CBS inhibition), downstream alterations (e.g., lack of production of cytoprotective cystathione or $H_2S$ after CBS inhibition) or global cellular changes (e.g., alterations in cellular glutathione levels and compensatory changes in redox balance)". Likewise, protein-protein interaction should be taken into the consideration, regarding the function. It was already published that silencing of the CBS in HCT116 cells decreases cell proliferation and attenuates HCT116 xenograft growth and vascularization in female Balb/c nude mice. These observations were performed either by silencing techniques, or by the CBS blockers, such as S-adenosyl-L-methionine [32] or aminooxyacetic acid [33], which did not allow the complete blockade of CBS. Using CRISPR/Cas9 approach one can ensure that CBS is permanently deleted. Also, we used positive and negative CRISPR controls to eliminate possible false results caused by CRISPR technology.

Transcription factor p53 plays an important role in preventing tumorigenesis and tumor progression [34]. Downregulation of phospho-p53 (Ser15) expression predicted poor prognosis in patients with colorectal carcinoma [35]. Although we could not comment about the levels of phospho-p53 in colorectal carcinoma DLD1 cells compared to non-tumor colon cells, we have clearly shown that in DLDx cells level of this phosphorylated protein is significantly decreased compared to DLD1 cells, thus pointing to increased tumorigenicity. Based on this results one might speculate that pathways upstream of phospho-p53 might be affected by $H_2S$. Further research is required to clarify this issue.

# Conclusion

In summary, we have shown that in colorectal carcinoma cells DLD1 cytoskeletal proteins b-actin and b-tubulin bind to CBS, which has an impact on tumor's growth, proliferation and migration. Although some beneficial effects by exogenous supplementation of $H_2S$ on tubulin organization and cell´s migration are shown, we still cannot convincingly conclude whether $H_2S$ is the crucial player in observed reorganization of cytoskeleton and modulation of tumorigenicity in colorectal carcinoma cells, or whether CBS realizes the above-mentioned effects through other upstream/downstream mechanisms. This will be the further direction in our research.

# Abbreviations

CBS: cystathionine-b-synthase; ccRCC: clear cell renal cell carcinoma; CRISPR: clustered, regularly interspaced, short palindromic repeats; DAPI: 4',6-diamidino-2-phenylindole; DATS: diallyl trisulfide; CHAPS: (3-[(3-cholamidopropyl) dimethylammonio] 1-propanesulfonate; $H_2S$: hydrogen sulfide; IF: Immunofluorescence PLA: Proximity ligation assay; sgRNA: single guide RNA; PTX: paclitaxel; TBS-T: Tris-buffered Saline with Tween-20; Vin: vincristine sulfate salt; WB: Western blot analysis

# Declarations

### Ethics approval and consent to participate

Animal experiments were approved by the Institutional Ethic Committee and by the national competence authority – State Veterinary and Food Administration of the Slovak Republic (project registration No. Ro-2032-3/2020-220) in compliance with the Directive 2010/63/EU and the Regulation 377/2012 on the protection of animals used for scientific purposes. Project was conducted in the approved animal facility (license No. SK UCH 02017).

**Consent for publication** Not applicable.

### Availability of data and materials

The datasets used and/or analysed during the current study are available from the corresponding author on reasonable request.

### Competing interests

The authors declare that they have no competing interests.

### Funding

This work was supported by grant from Ministry of Health, Slovak Republic nr. 2019/58-BMCSAV-2 and partially by grant APVV-16-0246. IncuCyte ZOOM Imaging system was sponsored by Slovak Cancer Research Foundation.

### Authors' contributions

Conception and design: OK. Development of methodology: VL, IR, MM. Acquisition of data: VL, BCH, PB, IR, KPP. Data analysis and interpretation: VL, BCH, PB, MM, OK. Writing of the manuscript: VL, MM, OK. Study supervision: OK. All authors have approved the manuscript.

### Acknowledgement

Authors wish to thank Mrs. Rojikova and Repaska for the help with animal experiments and prof. Cierna for quantification of Ki67 staining.

# References

1. Panagaki T, Randi EB, Augsburger F, Szabo C. Overproduction of $H_2S$, generated by CBS, inhibits mitochondrial Complex IV and suppresses oxidative phosphorylation in Down syndrome. Proc Natl Acad Sci USA. 2019;116:18769-71.
2. Zuhra K, Augsburger F, Majtan T, Szabo C. Cystathionine-β-synthase: molecular regulation and pharmacological inhibition. Biomolecules. 2020;10:697.
3. Weiss N, Heydrick S, Zhang YY, Bierl C, Cap A, Loscalzo J. Cellular redox state and endothelial dysfunction in mildly hyperhomocysteinemic cystathionine beta-synthase-deficient mice. Arterioscler Thromb Vasc Biol. 2002;22:34-41.
4. Comas F, Latorre J, Ortega F, Oliveras-Cañellas N, Lluch A, Ricart W, et al. Permanent cystathionine-β-synthase gene knockdown promotes inflammation and oxidative stress in immortalized human adipose-derived mesenchymal stem cells, enhancing their adipogenic capacity. Redox Biol. 2020;2:101668.
5. Fox B, Schantz J. T, Haigh R, Wood M. E, Moore P. K, Viner N, et al. Inducible hydrogen sulfide synthesis in chondrocytes and mesenchymal progenitor cells: is $H_2S$ a novel cytoprotective mediator in the inflamed joint? J Cell Mol Med. 2010;16:896-910.
6. Szabo C, Coletta C, Chao C, Módis K, Szczesny B, Papapetropoulos A, et al. Tumor-derived hydrogen sulfide, produced by cystathionine-β-synthase, stimulates bioenergetics, cell proliferation, and angiogenesis in colon cancer. Proc Natl Acad Sci USA. 2013;110:12474-9.

7. Yue T, Zuo S, Bu D, Zhu J, Chen S, Ma Y, et al. Aminooxyacetic acid (AOAA) sensitizes colon cancer cells to oxaliplatin via exaggerating apoptosis induced by ROS. J Cancer.2020;11:1828-38.
8. Breza J Jr, Soltysova A, Hudecova S, Penesova A, Szadvari I, Babula P, et al. Endogenous $H_2S$ producing enzymes are involved in apoptosis induction in clear cell renal cell carcinoma. BMC Cancer. 2018;18:591.
9. Guo H, Gai, JW, Wang Y, Jin HF, Du JB, Jin J. Characterization of hydrogen sulfide and its synthases, cystathionine β-synthase and cystathionine γ-lyase, in human prostatic tissue and cells. Urology. 2012;79:483-e1.
10. Turbat-Herrera EA, Kilpatrick MJ, Chen J, Meram AT, Cotelingam J, Ghali G, et al. Cystathione β-synthase is increased in thyroid malignancies. Anticancer Res. 2018;38:6085-90.
11. Dongsoo K, Chen J, Wei E, Ansari J, Meram A, Patel S, et al. Hydrogen sulfide and hydrogen sulfide-synthesizing enzymes are altered in a case of oral adenoid cystic carcinoma. Case Rep Oncol. 2018;11:585-90.
12. Cao X, Ding L, Xie ZZ, Yang Y, Whiteman M, Moore PK, et al. A Review of hydrogen sulfide synthesis, metabolism, and measurement: is modulation of hydrogen sulfide a novel therapeutic for cancer? Antioxid Redox Signal. 2019;11:1-38.
13. Szadvari I, Hudecova S, Chovancova B, Matuskova M, Cholujova D, Lencesova L et al. Sodium/calcium exchanger is involved in apoptosis induced by $H_2S$ in tumor cells through decreased levels of intracellular pH. Nitric Oxide. 2019;87:1-9.
14. Lu S, Gao Y, Huang X, Wang X. GYY4137, a hydrogen sulfide ($H_2S$) donor, shows potent anti-hepatocellular carcinoma activity through blocking the STAT3 pathway. Int J Oncol. 2014;44:1259-67.
15. Bhattacharyya S, Saha S, Giri K, Lanza IR, Nair KS, Jennings NB, et al. Cystathionine beta-synthase (CBS) contributes to advanced ovarian cancer progression and drug resistance. PLoS One. 2013;8:e79167.
16. Santos I, Ramos C, Mendes C, Sequeira CO, Tomé CS, Fernandes DGH, et al. Targeting glutathione and cystathionine β-Synthase in ovarian cancer treatment by selenium-chrysin polyurea dendrimer nanoformulation. Nutrients. 2019;11:2523.
17. Sen S, Kawahara B, Gupta D, Tsai R, Khachatryan M, Roy-Chowdhuri S, et al. Role of cystathionine β-synthase in human breast Cancer. Free Radic Biol Med. 2015;86:228-38.
18. Teng H, Wu B, Zhao K, Yang G, Wu L, Wang, R. Oxygen-sensitive mitochondrial accumulation of cystathionine β-synthase mediated by Lon protease. Proc Natl Acad Sci USA. 2013,110:12679-84.
19. Szabo C, Ransy C, Módis K, Andriamihaja M , Murghes B, Coletta C et al. Regulation of mitochondrial bioenergetic function by hydrogen sulfide. Part I. Biochemical and physiological mechanisms. Br J Pharmacol. 2014;171:2099-2122.
20. Parker AL, Teo WS, McCarroll JA, Kavallaris M. An emerging role for tubulin isotypes in modulating cancer biology and chemotherapy resistance. Int J Mol Sci. 2017;18:1434.

21. Chaudhuri AR, Khan IA, Luduena RF. Detection of disulfide bonds in bovine brain tubulin and their role in protein folding and microtubule assembly in vitro: A novel disulfide detection Approach. Biochemistry. 2001;40:8834-41.
22. Mustafa AK, Gadalla MM, Sen N, Kim S, Mu W, Gazi SK, et al. $H_2S$ signals through protein S-sulfhydration. Sci Signal. 2009;2:ra72.
23. Hosono T, Fukao T, Ogihara J, Ito Y, Shiba H, Seki T, et al. Diallyl trisulfide suppresses the proliferation and induces apoptosis of human colon cancer cells through oxidative modification of beta-tubulin. J Biol Chem. 2005;280:41487-93.
24. Steinmetz MO, Prota AE. Microtubule-targeting agents: strategies to hijack the cytoskeleton. Trends Cell Biol. 2018;28:776-92.
25. Sanjana NE, Shalem O, Zhang F. Improved vectors and genome-wide libraries for CRISPR screening. Nat Methods. 2014;11:783-4.
26. Shalem O, Sanjana NE, Hartenian E, Shi X, Scott DA, Mikkelson T, et al. Genome-scale CRISPR-Cas9 knockout screening in human cells. Science. 2014;343:84-7.
27. Borys F, Joachimiak E, Krawczyk H, Fabczak H. Intrinsic and extrinsic factors affecting microtubule dynamics in normal and cancer cells. Molecules. 2020;25:3705.
28. Schiff PB, Fant J, Horwitz SB. Promotion of microtubule assembly in vitro by taxol. Nature. 1979;277:665-7.
29. Britto PJ, Knipling L, McPhie P, Wolff J. Thiol-disulphide interchange in tubulin: kinetics and the effect on polymerization. Biochem J. 2005;389:549-58.
30. Britto PJ, Knipling L, Wolff J. The local electrostatic environment determines cysteine reactivity of tubulin. J Biol Chem. 2002;277:29018-27.
31. Li L, Whiteman M, Guan YY, Neo KL, Cheng Y, Lee SW, et al. Characterization of a novel, water-soluble hydrogen sulfide-releasing molecule (GYY4137). Circulation. 2008;117:2351-60.
32. Módis K, Coletta C, Asimakopoulou A, Szczesny B, Chao C, Papapetropoulos A, et al. Effect of S-adenosyl-L-methionine (SAM), an allosteric activator of cystathionine-β-synthase (CBS) on colorectal cancer cell proliferation and bioenergetics in vitro. Nitric Oxide. 2014;41:146-56.
33. Chao C, Zatarain JR, Ding Y, Coletta C, Mrazek AA, Druzhyna N et al. Cystathionine-β-synthase inhibition for colon cancer: enhancement of the efficacy of aminooxyacetic acid via the prodrug approach. Mol. Med. 2016;22:361-79.
34. Li Y, Wang Z, Chen Y, Petersen RB, Zheng L, Huang K. Salvation of the fallen angel: Reactivating mutant p53. Br. J. Pharmacol. 2019;176:6817-831.
35. Wang C, Liu S, Kuang Y, Hu X, Fang, X. Downregulation of ZNF365 by methylation predicts poor prognosis in patients with colorectal cancer by decreasing phospho-p53 (Ser15) expression. Oncol Lett. 2020;20:84.

# Figures

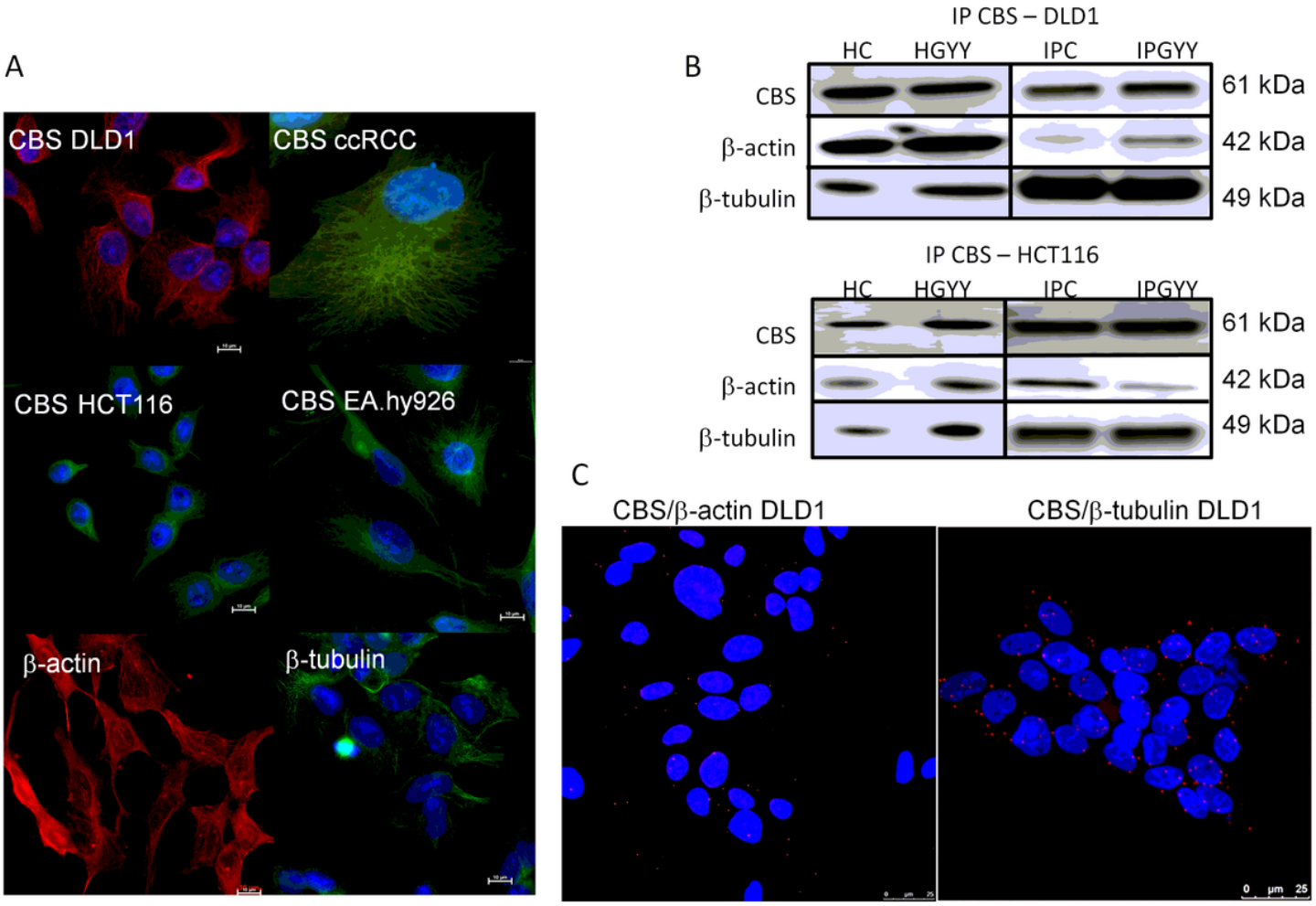


## Figure 1

Cystathionine-β-synthase (CBS) is bound to cell cytoskeleton. Immunofluorescence with CBS revealed that this enzyme has in various cells similar distribution pattern than β-actin and β-tubulin (A). Therefore, for further experiments we used colorectal carcinoma cells (DLD1) and we performed immunoprecipitation of CBS with subsequent detection of β-actin and β-tubulin (B) in control, untreated DLD1 and/or HCT116 cells and cells treated with a slow sulfide donor GYY4137 (GYY, 10 μM). We have seen a signal of both these proteins in immunoprecipitated sample. To verify the co-localizaton of CBS and β-actin/β-tubulin, we completed the proximity ligation assay (C), where we demonstrated a clear red signal showing co-localization of CBS with both cytoskeletal proteins. IP- immunoprecipitation, ccRCC - stable cell line derived from clear cell renal cell carcinoma, HCT116 - human colorectal carcinoma cell line, EA.hy926 – non-cancer endothelial cell line. For (A), scale bar represents 10 μm, for (C) 25 μm.

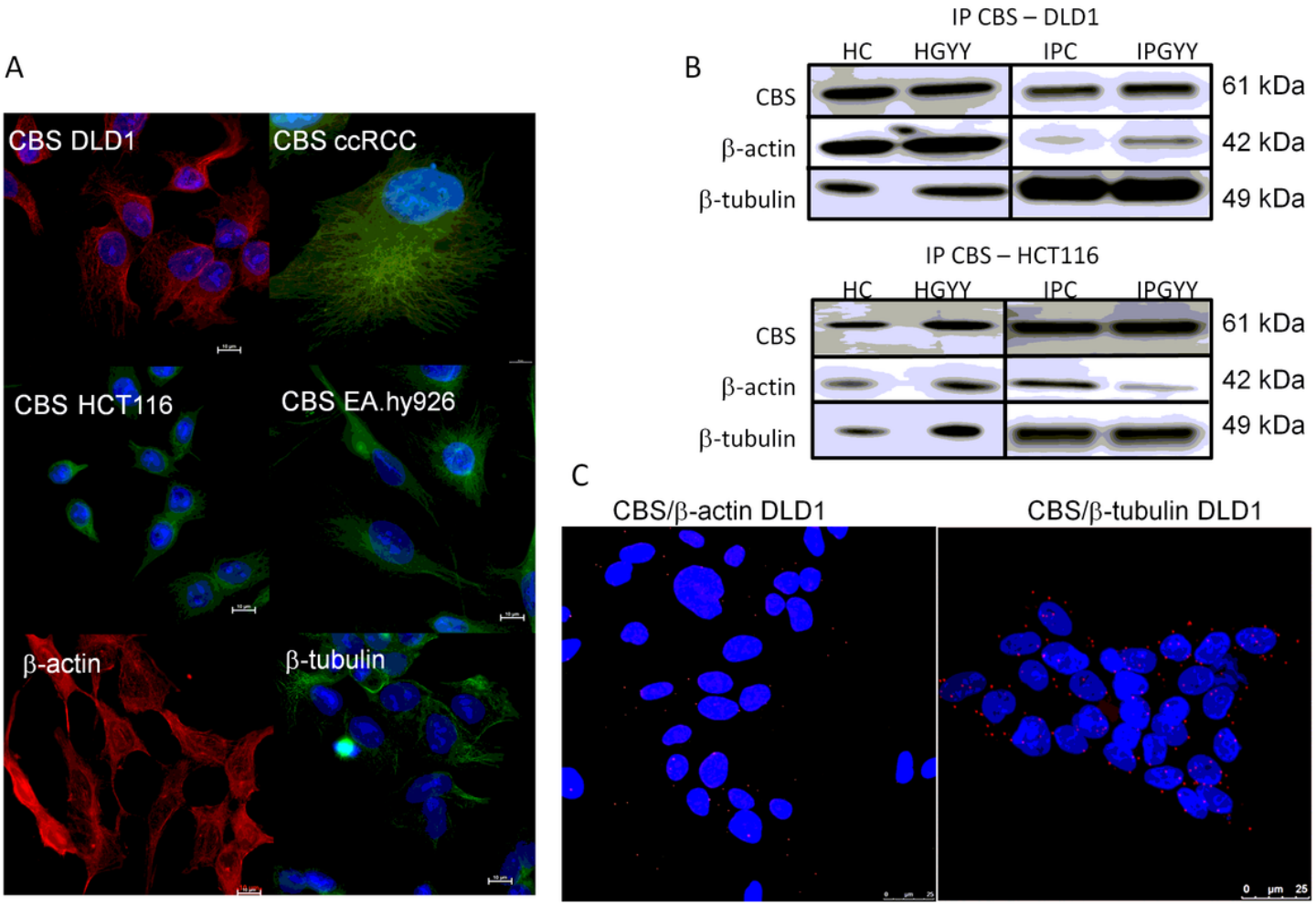


## Figure 1

Cystathionine-β-synthase (CBS) is bound to cell cytoskeleton. Immunofluorescence with CBS revealed that this enzyme has in various cells similar distribution pattern than β-actin and β-tubulin (A). Therefore, for further experiments we used colorectal carcinoma cells (DLD1) and we performed immunoprecipitation of CBS with subsequent detection of β-actin and β-tubulin (B) in control, untreated DLD1 and/or HCT116 cells and cells treated with a slow sulfide donor GYY4137 (GYY, 10 μM). We have seen a signal of both these proteins in immunoprecipitated sample. To verify the co-localizaton of CBS and β-actin/β-tubulin, we completed the proximity ligation assay (C), where we demonstrated a clear red signal showing co-localization of CBS with both cytoskeletal proteins. IP- immunoprecipitation, ccRCC - stable cell line derived from clear cell renal cell carcinoma, HCT116 - human colorectal carcinoma cell line, EA.hy926 – non-cancer endothelial cell line. For (A), scale bar represents 10 μm, for (C) 25 μm.

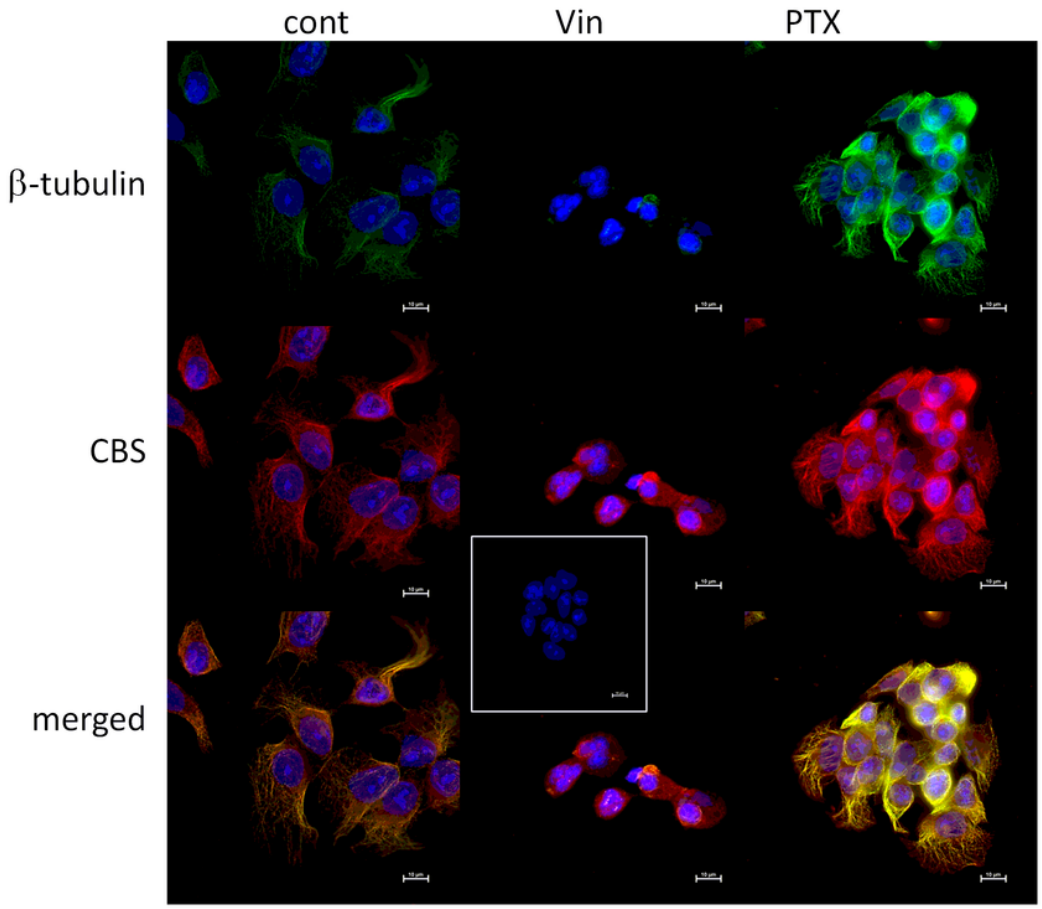


## Figure 2

Double immunofluorescence staining of β-tubulin (green) and cystathionine-β- synthase (CBS; red) in DLD1 cells in control conditions and also after the treatment with vincristine (Vin) and paclitaxel (PTX). Nuclei are stained with DAPI (blue). Compared to control untreated cells, in the presence of Vin the signals of β-tubulin and CBS were significantly suppressed, while in the presence of PTX both signals were boosted. Inset shows the negative control, where both primary antibodies were omitted. Scale bar represents 10 μm.

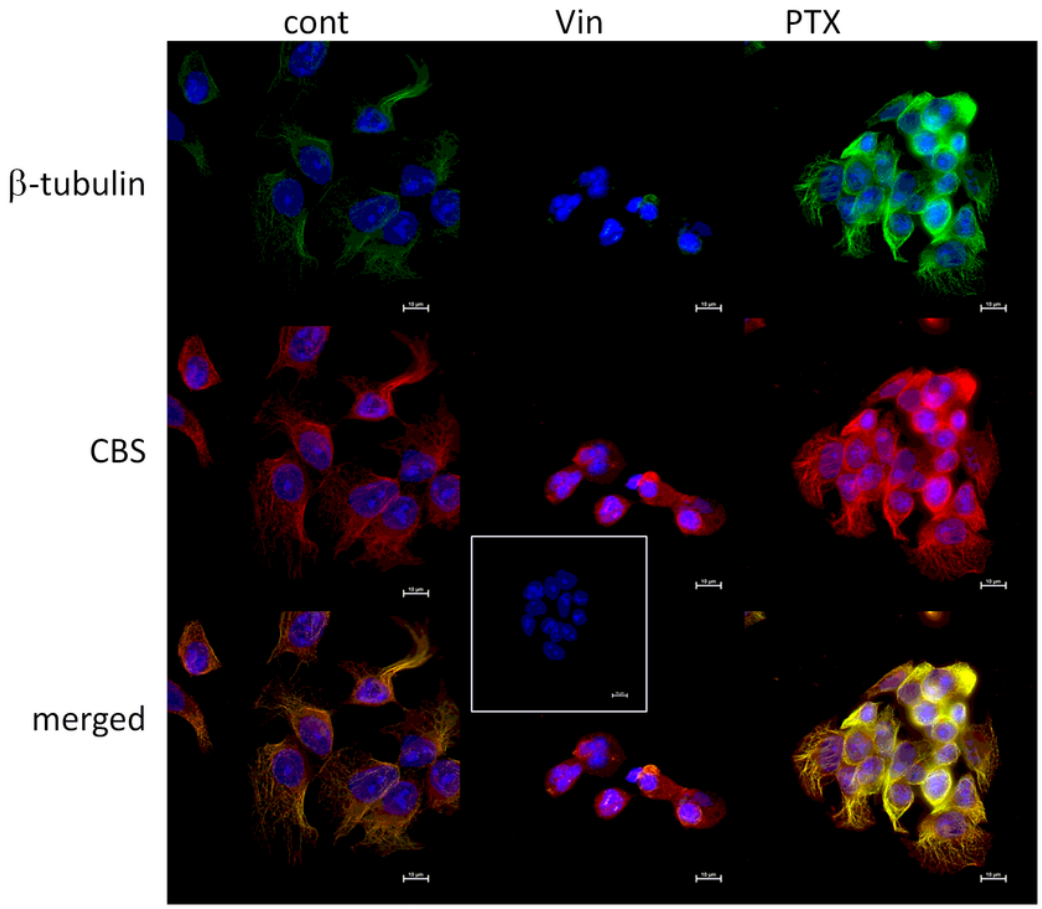


## Figure 2

Double immunofluorescence staining of β-tubulin (green) and cystathionine-β- synthase (CBS; red) in DLD1 cells in control conditions and also after the treatment with vincristine (Vin) and paclitaxel (PTX). Nuclei are stained with DAPI (blue). Compared to control untreated cells, in the presence of Vin the signals of β-tubulin and CBS were significantly suppressed, while in the presence of PTX both signals were boosted. Inset shows the negative control, where both primary antibodies were omitted. Scale bar represents 10 μm.

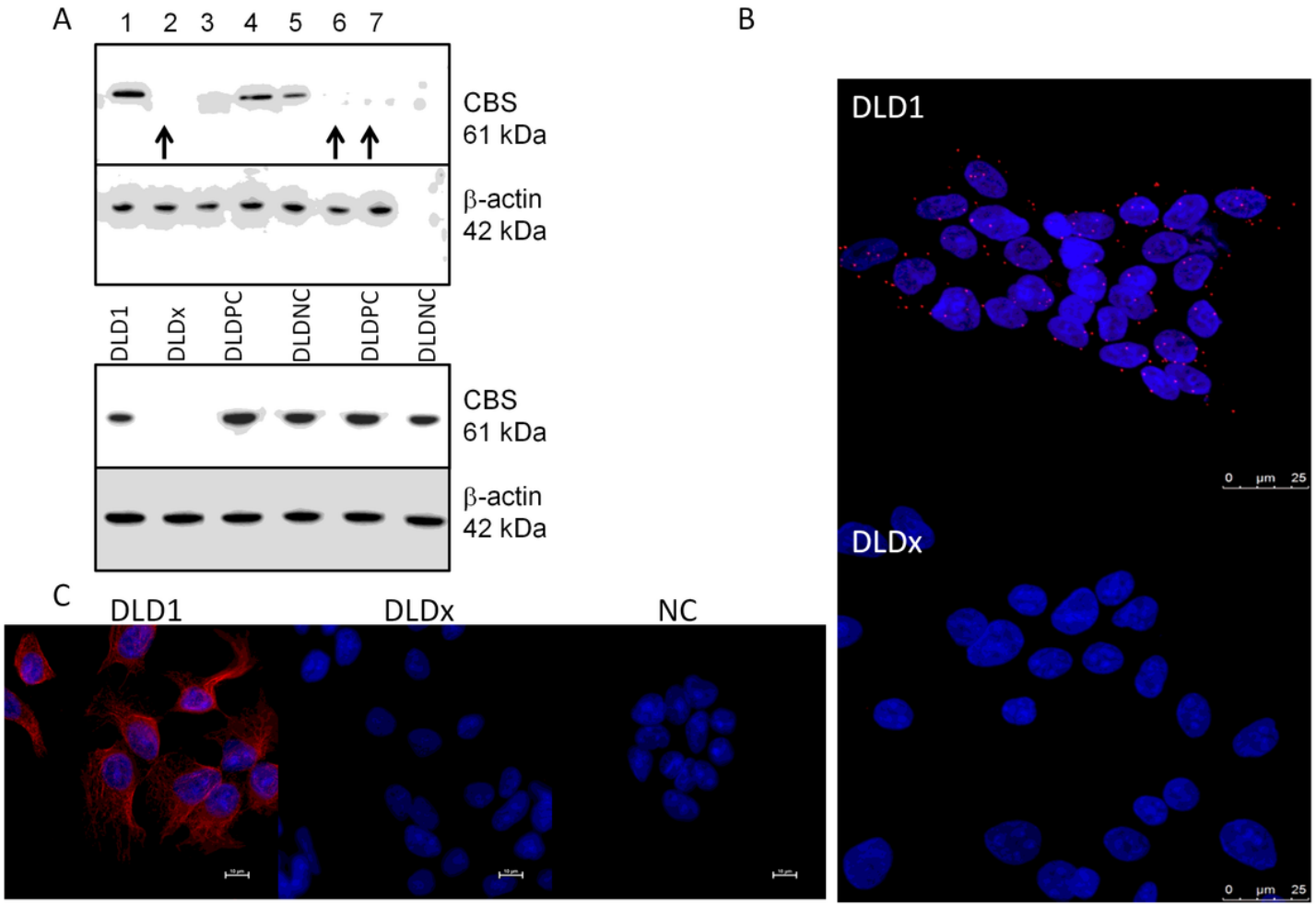


## Figure 3

Preparation of DLD1/CBS_del cell line (DLDx) using CRISPR/Cas9 gene editing method. This cell line was prepared as described in Material and Methods. Presence of CBS was tested by Western blot analysis (A), proximity ligation assay with β-tubulin and CBS antibodies (B) and immunofluorescence with CBS antibody (C). From seven clones tested after purification and puromycin selection three clones were lacking CBS (2,6 and 7). We used clone 2 for further experiments. We also prepared positive and negative CRISPR controls, as described in Material and Methods. CBS was present in positive (DLD-PC) and negative (DLD-NC) CRISPR controls. Proximity ligation assay revealed a nice co-localization signal of CBS and β-tubulin in unmodified DLD1 cells, however, in DLDx cells co-localization signal was missing. Immunofluorescence showed CBS signal in DLD1, but not in DLDx cells. All these experiments support the fact that CBS was knockouted in DLDx cells. For (B), scale bar represents 25 μm, for (C) 10 μm.

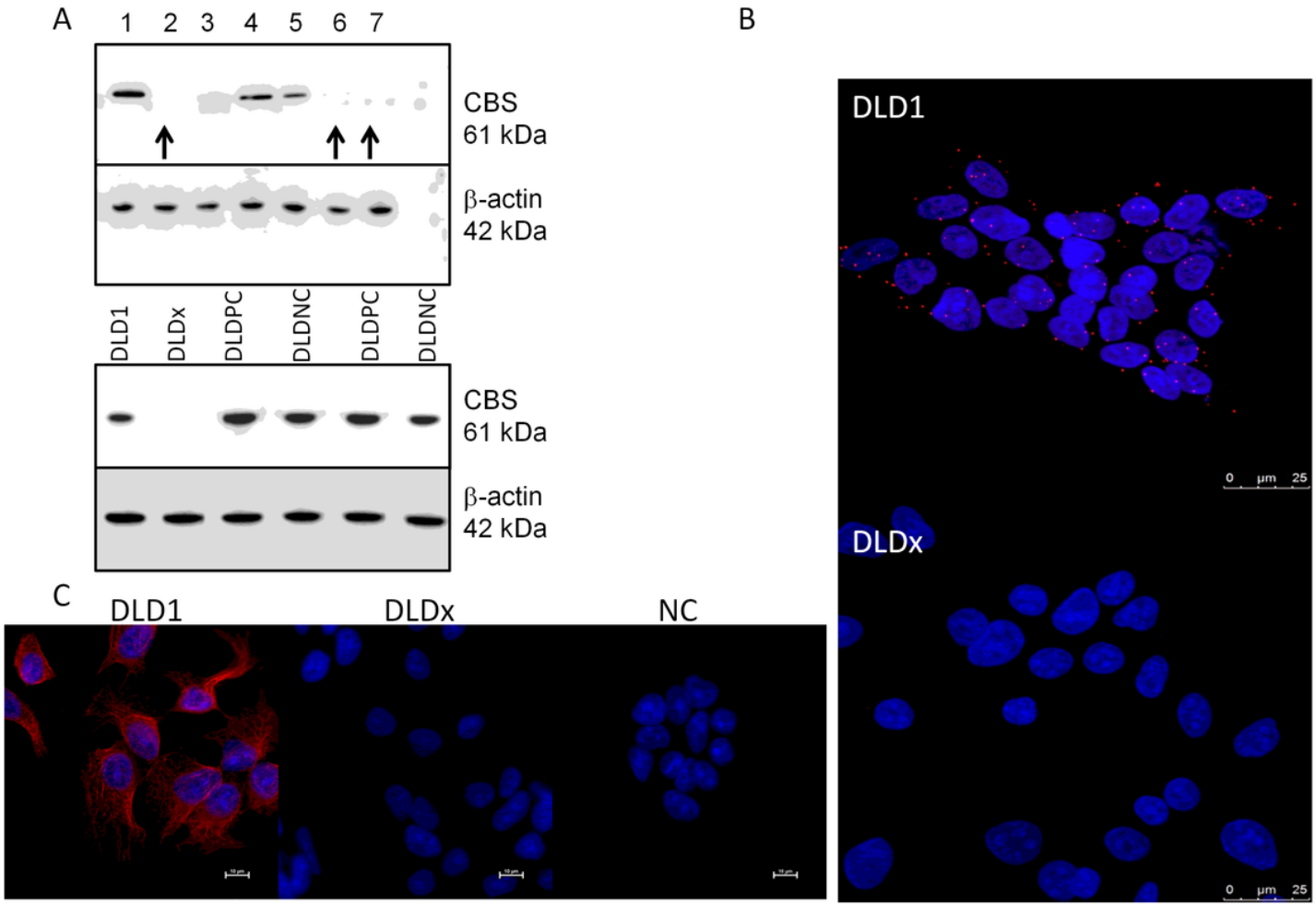


## Figure 3

Preparation of DLD1/CBS_del cell line (DLDx) using CRISPR/Cas9 gene editing method. This cell line was prepared as described in Material and Methods. Presence of CBS was tested by Western blot analysis (A), proximity ligation assay with β-tubulin and CBS antibodies (B) and immunofluorescence with CBS antibody (C). From seven clones tested after purification and puromycin selection three clones were lacking CBS (2,6 and 7). We used clone 2 for further experiments. We also prepared positive and negative CRISPR controls, as described in Material and Methods. CBS was present in positive (DLD-PC) and negative (DLD-NC) CRISPR controls. Proximity ligation assay revealed a nice co-localization signal of CBS and β-tubulin in unmodified DLD1 cells, however, in DLDx cells co-localization signal was missing. Immunofluorescence showed CBS signal in DLD1, but not in DLDx cells. All these experiments support the fact that CBS was knockouted in DLDx cells. For (B), scale bar represents 25 µm, for (C) 10 µm.

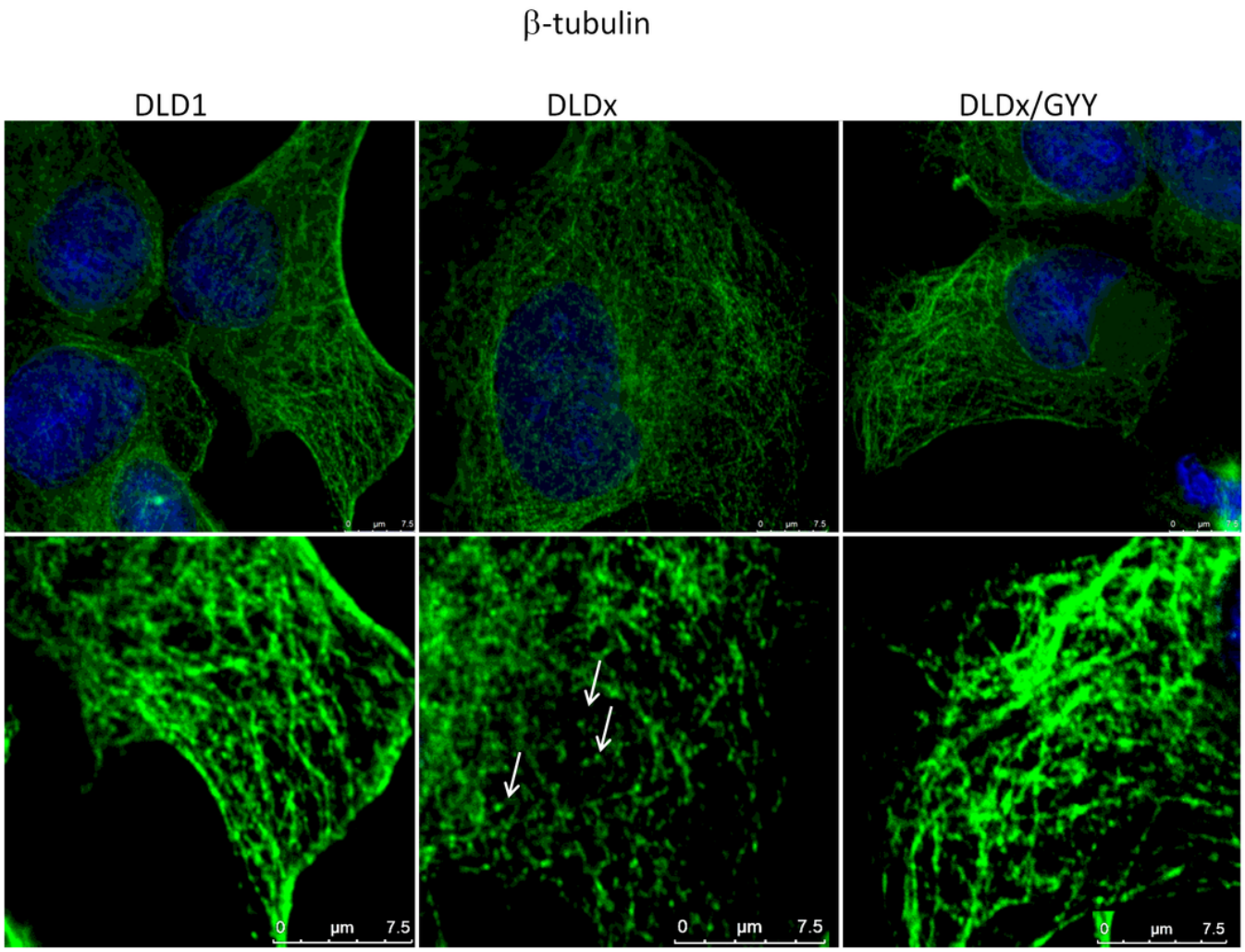


## Figure 4

Effect of H2S on microtubule structure. We compared β-tubulin morphology (green) in unmodified DLD1 cells, DLD1/CBS_del (DLDx) cell and also in DLDx cells treated with slow sulfide donor GYY4137 (GYY). In DLDx cells we observed partial re-modelation of β-tubulin skelet (e.g. showed by arrows). Interestingly, this skeleton became intact after GYY treatment. Nuclei were stained with DAPI. Scale bar represents 7.5 µm in both magnifications.

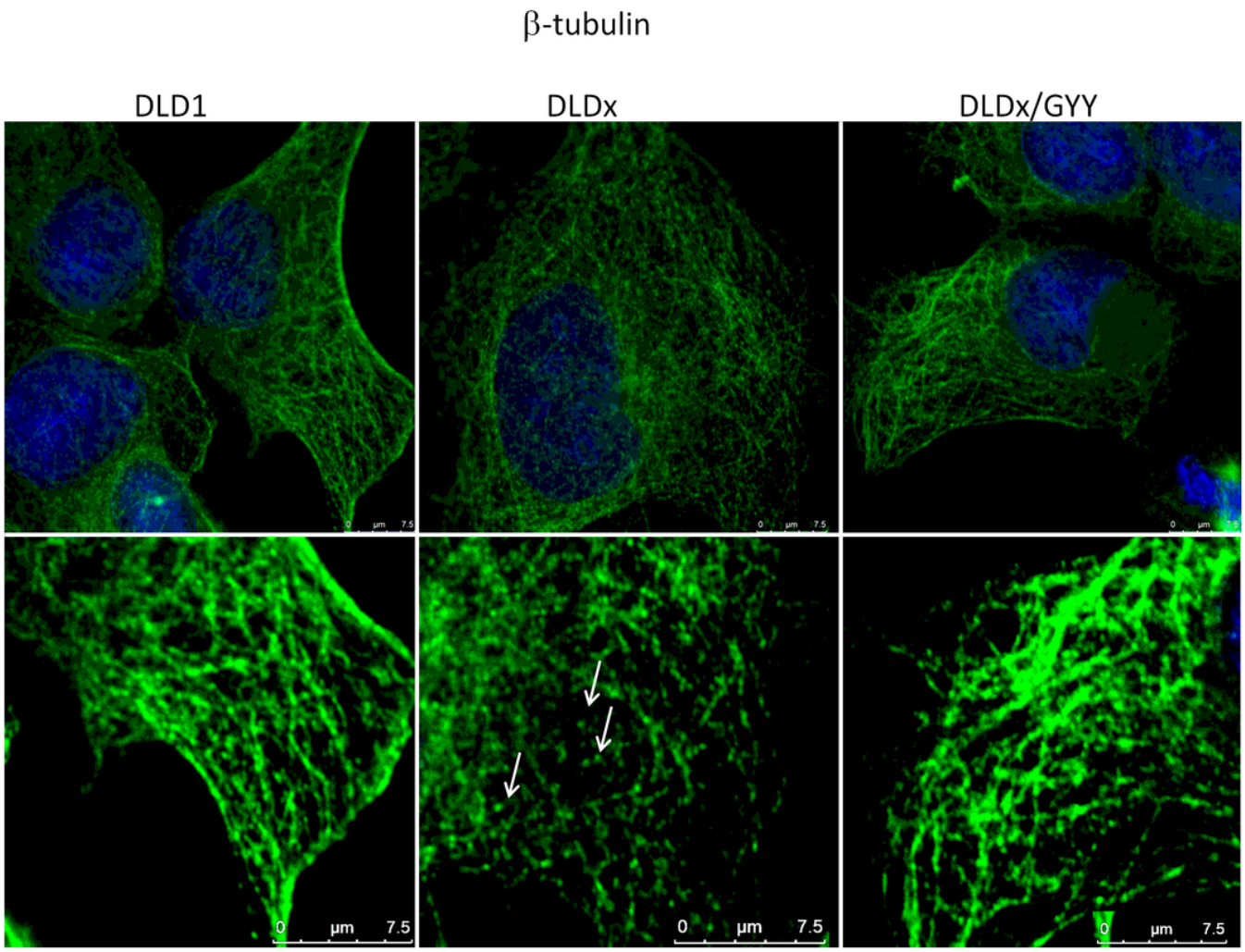


## Figure 4

Effect of H2S on microtubule structure. We compared β-tubulin morphology (green) in unmodified DLD1 cells, DLD1/CBS_del (DLDx) cell and also in DLDx cells treated with slow sulfide donor GYY4137 (GYY). In DLDx cells we observed partial re-modelation of β-tubulin skelet (e.g. showed by arrows). Interestingly, this skeleton became intact after GYY treatment. Nuclei were stained with DAPI. Scale bar represents 7.5 µm in both magnifications.

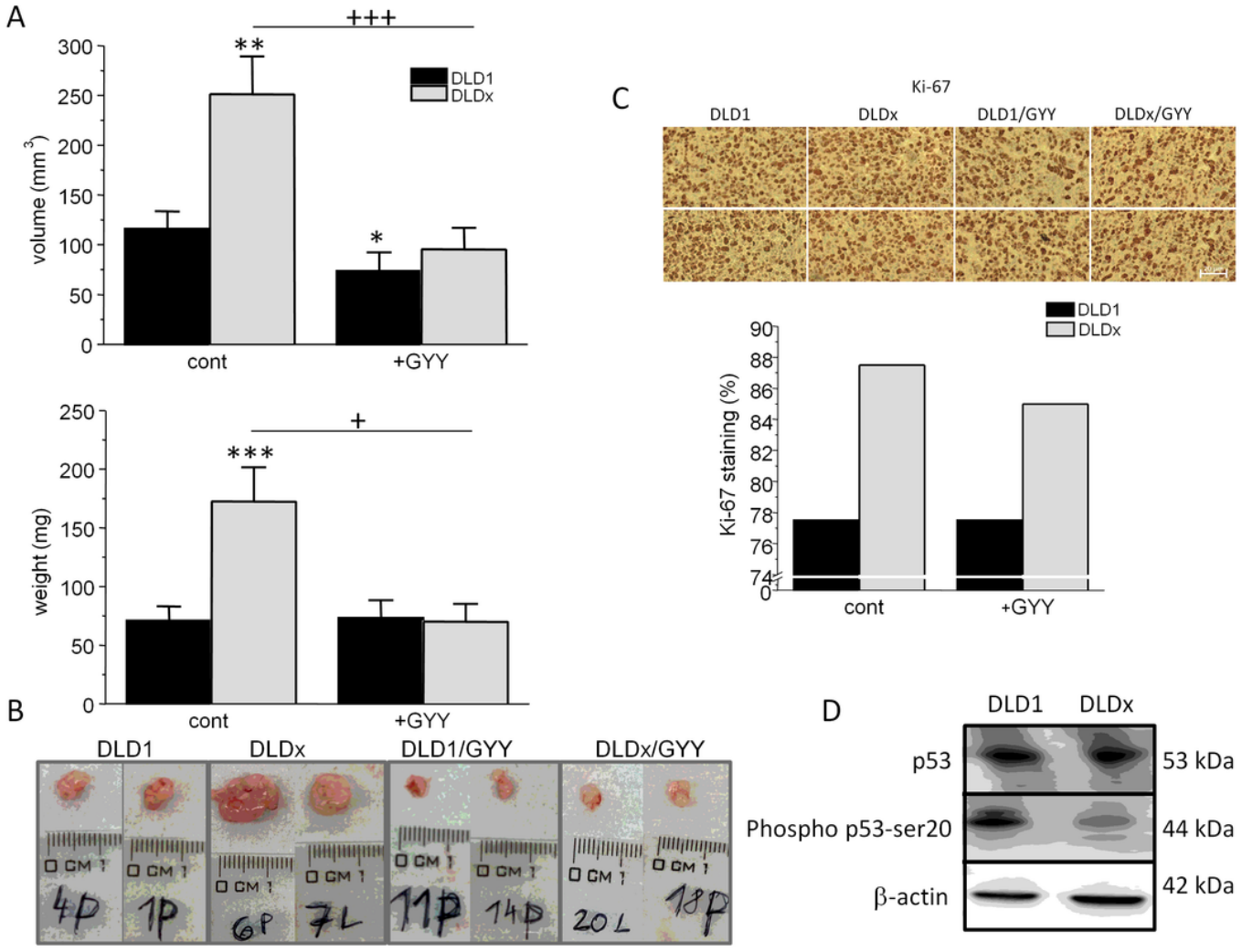


## Figure 5

Xenograft formation in SCID/bg mice inoculated by DLD1 and DLDx cells. Immunodeficient SCID/bg mice were inoculated by either DLD1, or DLDx (with knockouted CBS). On the fourth day, when small tumors started to be visible, mice were divided into four groups. One of two DLD1 groups and one of two DLDx groups was simultaneously treated with GYY4137 (GYY). On termination day 14, animals were sacrificed and the xenograft's volume (A,B) and weight of tumors (A) were estimated. Xenografts from DLDx cells were approximately twice as big in volume and weight compared to those from DLD1 cells. When mice were simultaneously treated with GYY, no significant difference in xenograft´s mass was observed from DLD1 cells inoculation, although significant decrease in volume occurred in tumors from these cells. Volume and mass of tumors in GYY treated DLDx mice was significantly smaller (A, B). Typical tumors from each group are shown in part (B). Positive and negative CRISPR controls did not affect size and/or volume of tumors, compared to DLD1 group (not shown). Proliferation marker Ki-67 was increased in xenografts from DLDx cells, in comparison to DLD1 cells (C). After GYY treatment, tumors from DLDx cells showed slightly decreased proliferation, compared to untreated cells. In DLDx cells, tumor suppressor phospho p53-ser20 was decreased in DLDx, compared to DLD1 cells (D). Results

are displayed as mean ± S.E.M., number of tumors evaluated n=10, for Ki-67 n=5. Statistical significance * - p< 0.05 and ** represents p< 0.01 compared to control DLD1 group. Statistical significance + p< 0.05 and +++ represents p< 0.001 compared to control DLDx group (A). Scale bar represents 20 μm (C).

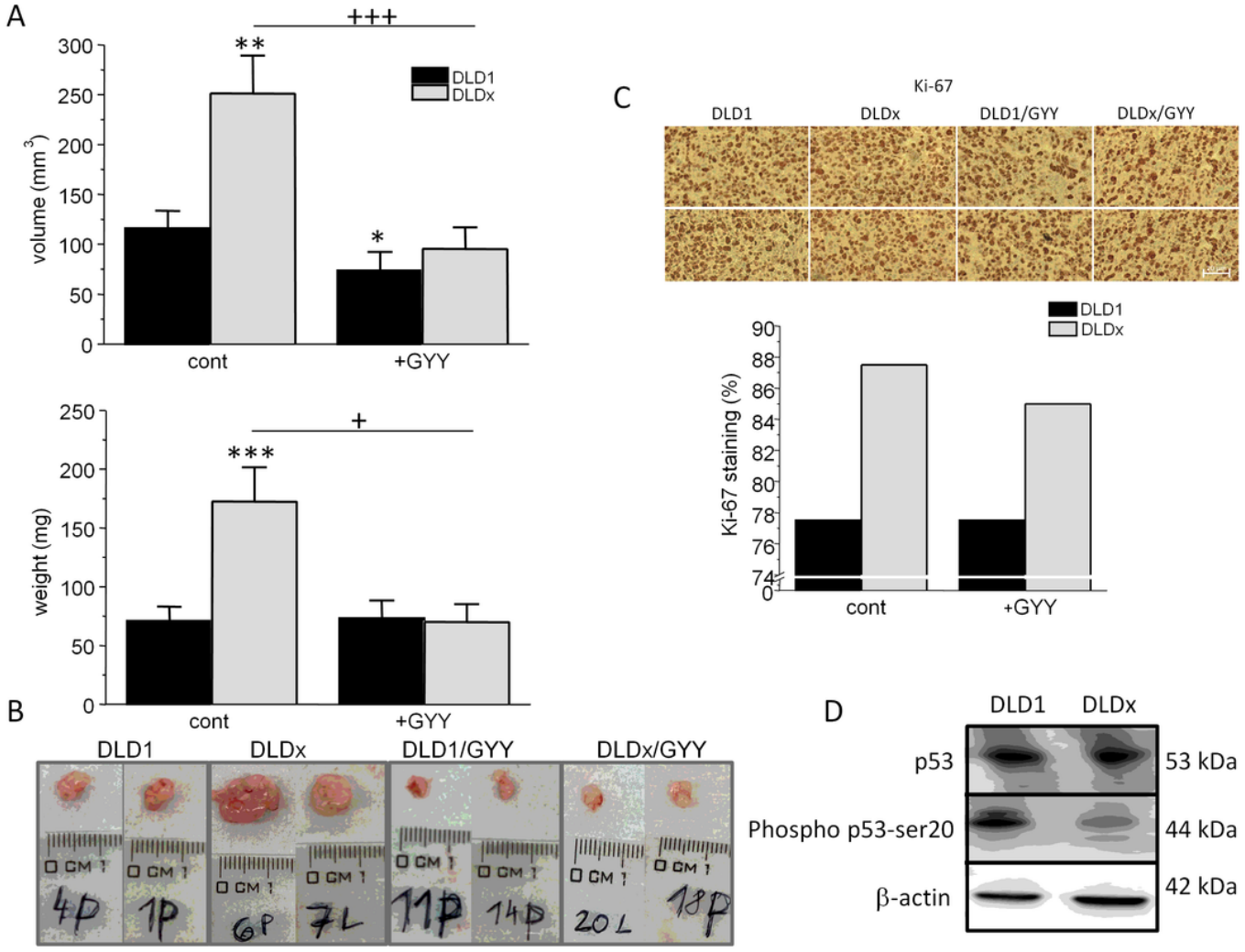


## Figure 5

Xenograft formation in SCID/bg mice inoculated by DLD1 and DLDx cells. Immunodeficient SCID/bg mice were inoculated by either DLD1, or DLDx (with knockouted CBS). On the fourth day, when small tumors started to be visible, mice were divided into four groups. One of two DLD1 groups and one of two DLDx groups was simultaneously treated with GYY4137 (GYY). On termination day 14, animals were sacrificed and the xenograft's volume (A,B) and weight of tumors (A) were estimated. Xenografts from DLDx cells were approximately twice as big in volume and weight compared to those from DLD1 cells. When mice were simultaneously treated with GYY, no significant difference in xenograft´s mass was observed from DLD1 cells inoculation, although significant decrease in volume occurred in tumors from these cells. Volume and mass of tumors in GYY treated DLDx mice was significantly smaller (A, B). Typical tumors from each group are shown in part (B). Positive and negative CRISPR controls did not affect size and/or volume of tumors, compared to DLD1 group (not shown). Proliferation marker Ki-67

was increased in xenografts from DLDx cells, in comparison to DLD1 cells (C). After GYY treatment, tumors from DLDx cells showed slightly decreased proliferation, compared to untreated cells. In DLDx cells, tumor suppressor phospho p53-ser20 was decreased in DLDx, compared to DLD1 cells (D). Results are displayed as mean ± S.E.M., number of tumors evaluated n=10, for Ki-67 n=5. Statistical significance * - p< 0.05 and ** represents p< 0.01 compared to control DLD1 group. Statistical significance + p< 0.05 and +++ represents p< 0.001 compared to control DLDx group (A). Scale bar represents 20 μm (C).

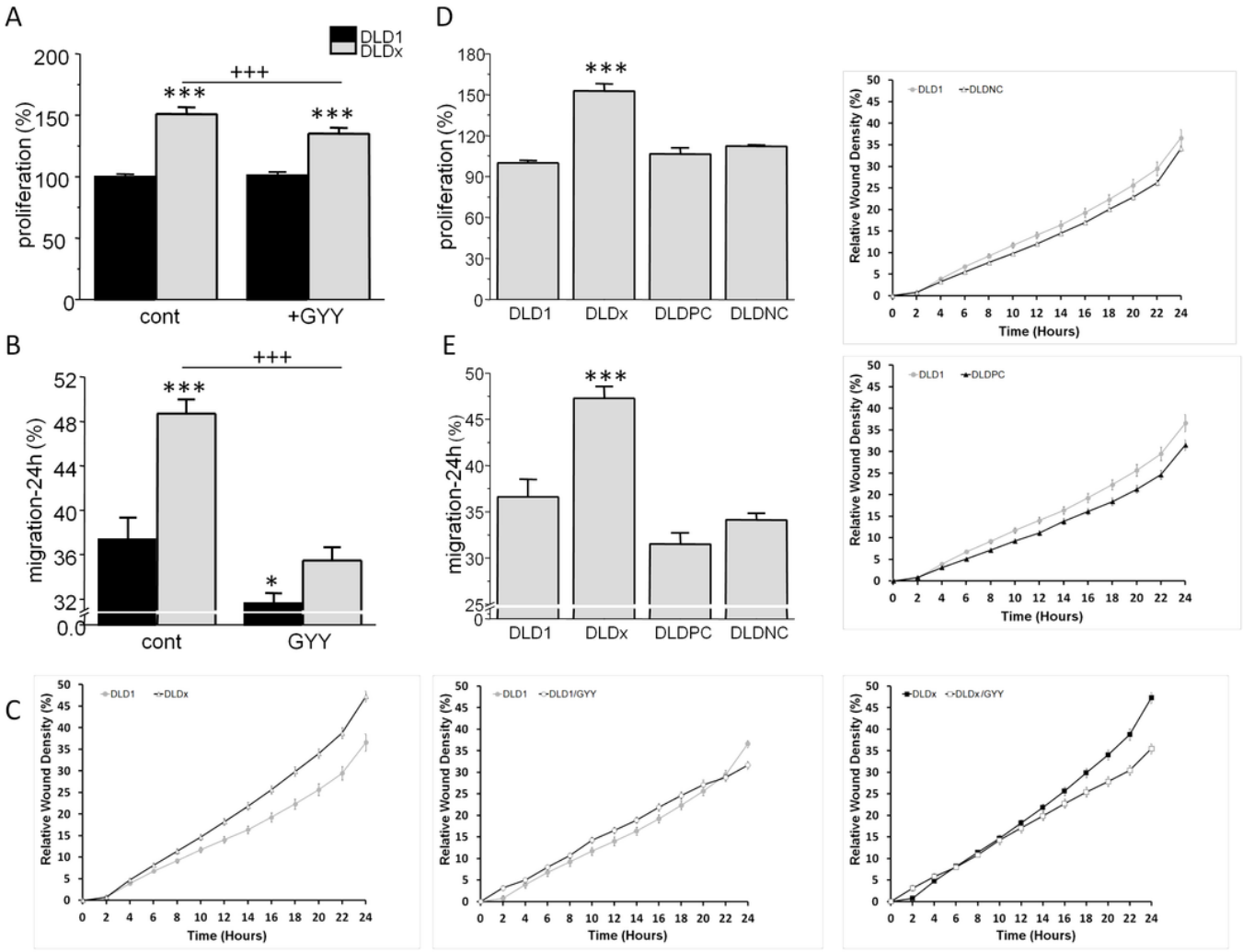


## Figure 6

Differences in proliferation (A) and migration (B,C) between control and GYY4137 (GYY) treated DLD1 and DLDx cells. Both, proliferation and migration were higher in DLDx compared to DLD1 cells. After a treatment with GYY, proliferation was not affected in DLD1 cell, but it was significantly decreased in DLDx cells (A). Migration was decreased in both, DLD1 and DLDx after GYY treatment (B). Typical result of migration curves is shown in (C). Positive and negative CRISPR controls did not affect proliferation and/or migration (D,E). Results are displayed as mean ± S.E.M. For proliferation, n=50, for migration, n= 20, for positive and negative controls n=15. Statistical significance *** represents p< 0.001 compared to

control DLD1 group. Statistical significance ++ - p< 0.01 and +++ represents p< 0.001 compared to control DLDx group.

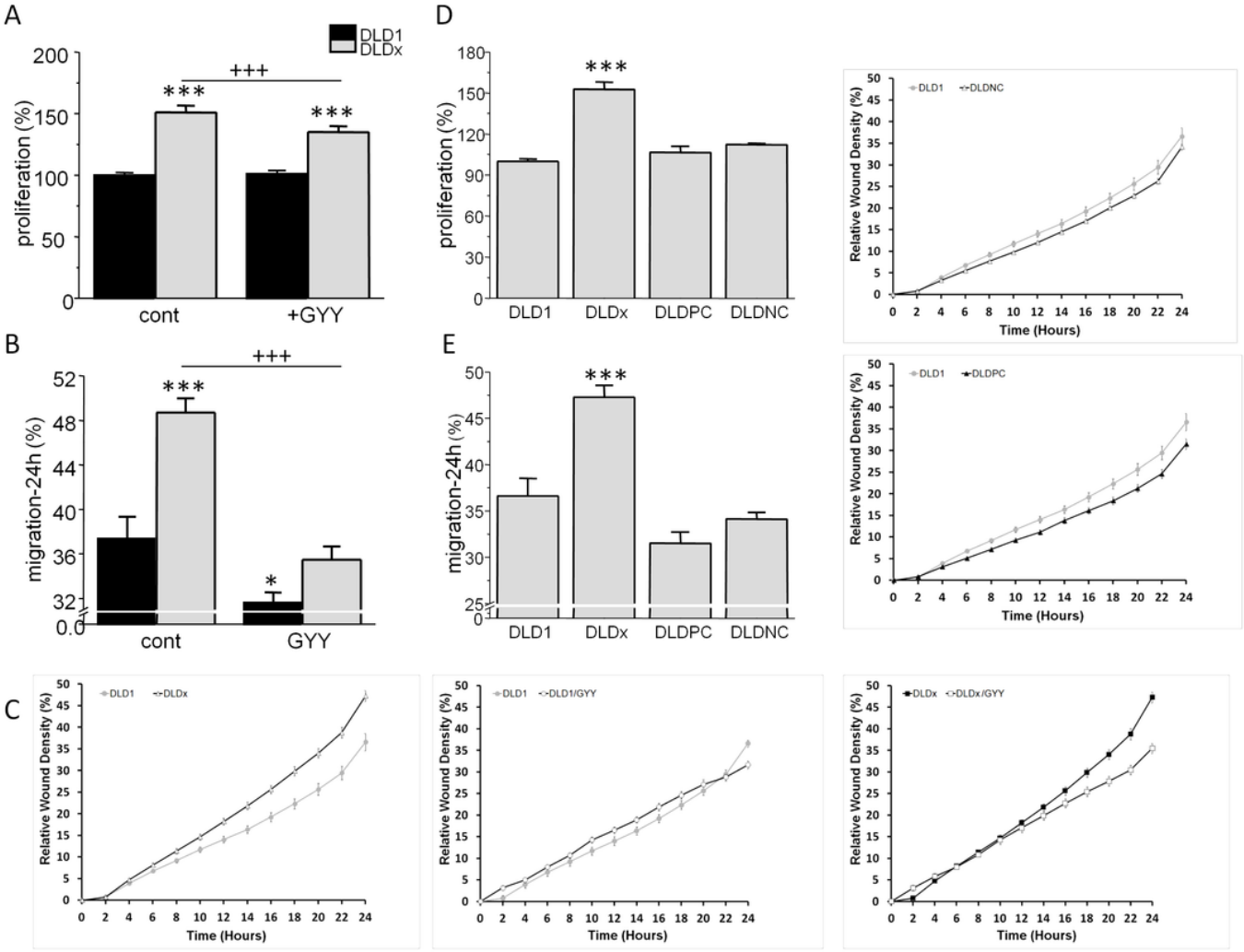


## Figure 6

Differences in proliferation (A) and migration (B,C) between control and GYY4137 (GYY) treated DLD1 and DLDx cells. Both, proliferation and migration were higher in DLDx compared to DLD1 cells. After a treatment with GYY, proliferation was not affected in DLD1 cell, but it was significantly decreased in DLDx cells (A). Migration was decreased in both, DLD1 and DLDx after GYY treatment (B). Typical result of migration curves is shown in (C). Positive and negative CRISPR controls did not affect proliferation and/or migration (D,E). Results are displayed as mean ± S.E.M. For proliferation, n=50, for migration, n= 20, for positive and negative controls n=15. Statistical significance *** represents p< 0.001 compared to control DLD1 group. Statistical significance ++ - p< 0.01 and +++ represents p< 0.001 compared to control DLDx group.